SCIENTIFIC REPORTS

OPEN

SUBJECT AREAS:
CLIMATE-CHANGE ECOLOGY
ECOSYSTEM ECOLOGY

Received
14 November 2014

Accepted
3 February 2015

Published
5 March 2015

Correspondence and requests for materials should be addressed to R.H. (horwitzrael@gmail.com)

Natural high pCO_2 increases autotrophy in *Anemonia viridis* (Anthozoa) as revealed from stable isotope (C, N) analysis

Rael Horwitz[1,3], Esther M. Borell[3], Ruth Yam[2], Aldo Shemesh[2] & Maoz Fine[1,3]

[1]The Mina and Everard Goodman Faculty of Life Sciences, Bar-Ilan University, Ramat-Gan 5290002, Israel, [2]Department of Earth and Planetary Sciences, Weizmann Institute of Science, Rehovot 7610001, Israel, [3]The Interuniversity Institute for Marine Sciences, P.O. Box 469, Eilat 8810300, Israel.

Contemporary cnidarian-algae symbioses are challenged by increasing CO_2 concentrations (ocean warming and acidification) affecting organisms' biological performance. We examined the natural variability of carbon and nitrogen isotopes in the symbiotic sea anemone *Anemonia viridis* to investigate dietary shifts (autotrophy/heterotrophy) along a natural pCO_2 gradient at the island of Vulcano, Italy. $\delta^{13}C$ values for both algal symbionts (*Symbiodinium*) and host tissue of *A. viridis* became significantly lighter with increasing seawater pCO_2. Together with a decrease in the difference between $\delta^{13}C$ values of both fractions at the higher pCO_2 sites, these results indicate there is a greater net autotrophic input to the *A. viridis* carbon budget under high pCO_2 conditions. $\delta^{15}N$ values and C/N ratios did not change in *Symbiodinium* and host tissue along the pCO_2 gradient. Additional physiological parameters revealed anemone protein and *Symbiodinium* chlorophyll *a* remained unaltered among sites. *Symbiodinium* density was similar among sites yet their mitotic index increased in anemones under elevated pCO_2. Overall, our findings show that *A. viridis* is characterized by a higher autotrophic/heterotrophic ratio as pCO_2 increases. The unique trophic flexibility of this species may give it a competitive advantage and enable its potential acclimation and ecological success in the future under increased ocean acidification.

Increasing carbon dioxide (CO_2) emissions drive ongoing ocean acidification (OA) and place marine ecosystems in a vulnerable state[1]. Predictions warn of a further decrease of 0.3–0.5 pH units in oceanic surface water by the end of this century[2]. Natural CO_2 vents at sub-tropical coastal areas[3–5] and tropical reefs[6] serve as natural laboratory locations to study long-term effects of elevated pCO_2 (pH) across many biological and spatial scales. Such a location has been reported in the Levante Bay of Vulcano Island (Italy) in the Mediterranean Sea where many studies have examined physiological adaptations of biota to OA, including seagrass[7], benthic micro- and macroalgaes[8,9], sea urchins[10], and sea anemones[11,12]. The distinctive characteristics of this location render it a unique environmental setting where the seawater chemistry varies along a pCO_2 gradient of several hundred meters moving away from the venting source. The submarine gas emissions in Levante Bay are characterized by high CO_2 content volume (>90%) and variable low H_2S (ranging 0.8 to 2.5% volume)[13].

A large body of research has focused on the potential impact of OA on reef organisms, particularly scleractinian corals. However, non-calcifying cnidarians such as sea anemones have received less attention[14]. Like many cnidarians, they are mixotrophic organisms, which derive their energy from both photoassimilates translocated from the dinoflagellate symbionts (*Symbiodinium*) and from a variety of external food sources[15]. *Symbiodinium* utilize bicarbonate (HCO_3^-), rather than $CO_{2(aq)}$, as the primary source for photosynthesis[16]. Extrinsic sources of carbon for the host include zooplankton and particulate organic carbon (POC)[17]. The two partners that make up the holobiont interact at the basic metabolic level, which includes reciprocal fluxes of energy and nutrient-rich compounds[18]. *Anemonia viridis* Forskål (Cnidaria: Anthozoa), the temperate Mediterranean species chosen for this study, occurs naturally at high densities throughout Levante Bay and harbors the dinoflagellate *Symbiodinium muscatinei* LaJeunesse and Trench (Dinomastigota: Dinophyceae)[12]. Hence it is a powerful comparative model to assess the effects of the changing seawater environment along a natural pCO_2 gradient.

Other reports on the response of *A. viridis* near CO_2 vents discovered changes in their associated microbial communities[19], reduced dimethylsulfoniopropionate (DMSP) production[12] and enhanced productivity[3,11].

The purpose of this paper is to investigate dietary changes of *A. viridis* using isotopic compositions, particularly carbon source shifts in the anemone metabolism, in response to high pCO_2/low pH conditions *in situ*. We measured how the natural variability of carbon and nitrogen isotopes in *Symbiodinium* and host tissues of *A. viridis* varies along a natural pCO_2 gradient. This was compared with other key physiological parameters (i.e. total protein concentration; *Symbiodinium* density, mitotic index, and chlorophyll concentration) which were used in the present and in previous studies[11]. Since the $\delta^{13}C$ and $\delta^{15}N$ signatures of an organism are related to those of its diet[20–24], our main objective was to estimate the relative contribution of photosynthetic compounds *versus* heterotrophically derived food to the anemone energetic budget (autotrophic/heterotrophic ratio) with increasing seawater pCO_2. This may facilitate better understanding of the environmental fate of cnidarians in a high CO_2 world.

Results

Visual observations made during the course of sampling found anemones at all sampling sites attached to hard substratum at high abundances (of ca. 10–40 anemones m^{-2}), consistent with previous findings[11]. Anemones appeared to be healthy with their tentacles fully extended and no visible excess amounts of mucus at the high pCO_2 site (Fig. 1b). Data for seawater pH, pCO_2, TA, temperature and light intensity at all anemone sampling sites is summarized in Figure 1a.

Total protein, *Symbiodinium* density, mitotic index and chlorophyll concentration. There was no significant difference in anemone protein concentration [1-way ANOVA: $F(2, 45) = 1.438$, $P = 0.248$] (Fig. 2a), *Symbiodinium* density [1-way ANOVA: $F(2, 45) = 0.583$, $P = 0.562$] and cell chlorophyll *a* concentration [1-way ANOVA: $F(2, 45) = 1.125$, $P = 0.334$] between sites (Fig. 2b). Mean protein concentration (mg protein g^{-1} wet wt ± SE) between sites was 37.65 ± 1.12. *Symbiodinium* density (cells mg $protein^{-1}$ ± SE) between sites averaged to 1.06 ± 0.07 × 10^6 and mean chlorophyll *a* content (pg $cell^{-1}$ ± SE) was 4.57 ± 0.27. The number of dividing *Symbiodinium* cells (MI) was progressively greater in anemones inhabiting the higher pCO_2 sites [1-way ANOVA: $F(2, 21) = 3.722$, $P = 0.041$], increasing from 3.69 ± 0.76% at the control site to 7.12 ± 1.44% and 9.8 ± 0.54% at the intermediate and high pCO_2 sites, respectively (Fig. 2c).

Seawater isotopic signature. Stable isotope analysis showed constant $\delta^{18}O_{seawater}$ between all sites, including the primary vent (Kruskal-Wallis ANOVA: df = 3, P = 0.361), with an average of 0.98 ± 0.01‰ (Fig. 3; vent site value not shown). $\delta^{13}C_{DIC}$ values were similar between sites 1–3, with an average of 1.28 ± 0.05‰ (Fig. 3), although all were significantly heavier compared to the primary vent site (0.34 ± 0.03‰) (Fig. 1a) (Kruskal-Wallis ANOVA: df = 3, P = 0.016).

$\delta^{13}C$ variability. $\delta^{13}C$ values of both animal tissue ($\delta^{13}C_T$) and *Symbiodinium* ($\delta^{13}C_S$) decreased under high pCO_2 conditions (Fig. 4a, b). One-way ANOVA revealed a significant difference in $\delta^{13}C_T$ between all sampling sites [$F(2, 12) = 42.901$, $P = 0.000003$], with a decrease from −16.66 ± 0.2‰ at the control site to −17.62 ± 0.19‰ and −19.12 ± 0.16‰ at the intermediate and high pCO_2 sites, respectively. $\delta^{13}C_S$ also differed significantly between all sampling sites [1-way ANOVA: $F(2, 12) = 25.606$, $P = 0.000047$], decreasing from −15.1 ± 0.28‰ at the control site to −16.65 ± 0.37‰ and −18.21 ± 0.24‰ at the intermediate and high pCO_2 sites, respectively. The difference in $\delta^{13}C$ between the anemone tissue ($\delta^{13}C_T$) and *Symbiodinium* ($\delta^{13}C_S$) at each site was calculated as $\delta^{13}C_S$- $\delta^{13}C_T$ to evaluate changes in autotrophic/heterotrophic ratios. $\delta^{13}C_T$ was considerably lighter than $\delta^{13}C_S$ at all sampling sites with $\delta^{13}C_S$- $\delta^{13}C_T$ reduced with increasing pCO_2 (Fig. 4a). In ambient seawater (control) this difference was relatively large (1.56 ± 0.21‰), while it decreased significantly at the intermediate and high pCO_2 sites (0.96 ± 0.31‰ and 0.9 ± 0.17‰, respectively) [1-way ANOVA: $F(2, 12) = 5.036$, $P = 0.026$].

$\delta^{15}N$ variability and C/N ratios. There was no significant difference in $\delta^{15}N$ values of anemone tissue ($\delta^{15}N_T$) [1-way ANOVA: $F(2, 12) = 0.848$, $P = 0.452$] and *Symbiodinium* ($\delta^{15}N_S$) [1-way ANOVA: $F(2, 12) = 0.266$, $P = 0.771$] with increasing pCO_2 (Fig. 5a). $\delta^{15}N_T$ was lowest at the control site (4.32 ± 0.12‰) and increased to 4.55 ± 0.16‰ and 4.6 ± 0.18‰ at the intermediate and high pCO_2 sites, respectively. $\delta^{15}N_S$ averaged to 1.34 ± 0.36 at the control site and increased to 1.41 ± 0.42 and 1.82 ± 0.41 at the intermediate and high pCO_2 sites, respectively. $\delta^{15}N_S$ was substantially lighter compared to $\delta^{15}N_T$ at all sampling sites, with an average difference of 2.5 ± 0.23‰ (Fig. 5a). The carbon to nitrogen ratios (C/N) of anemone tissue and *Symbiodinium* did not have any significant differences along the pCO_2 gradient (1-way ANOVAs; $F(2, 12) = 0.301$, $P = 0.745$ for anemone tissue; $F(2, 12) = 0.069$, $P = 0.934$ for *Symbiodinium*) (Fig. 5b). The C/N ratio of anemone tissue at the control site was 5.53 ± 0.36 and increased to 5.73 ± 0.21 and 5.91 ± 0.22 at the intermediate and high pCO_2 sites, respectively. The C/N ratio of *Symbiodinium* ranged from 7.34 ± 0.7 at the control site to 7.21 ± 0.51 at the high pCO_2 site.

Discussion

A. viridis collected at all pCO_2 sites lacked any apparent signs of stress (i.e. no mucus, tentacles fully extended; see Fig. 1b). Their general health was further supported by our results for physiological and algal characteristics. Protein concentrations, which are widely accepted as a sensitive indicator for the health of an organism[25], showed no difference between sampling sites, indicating *A. viridis* was in fact well acclimated to the high seawater pCO_2 (Fig. 2a). In addition, there were no changes in *Symbiodinium* densities and their chlorophyll *a* concentrations along the pCO_2 gradient (Fig. 2b). This is in agreement with observations of the anemone *Anthopleura elegantissima*, following exposure to elevated pCO_2 conditions in a laboratory setting, using the standard algal cell normalization to mg of protein methodology as in the present study[14]. However, *Symbiodinium* densities in *A. viridis* under high pCO_2 conditions nearby the vent at Vulcano have been reported to increase relative to algal densities in anemones at the control site[11]. This discrepancy may be the result of a different methodology (using surface area as a normalization index in the same study[11]) in determining algal cell densities. The handling of anemones greatly influences tentacle contraction, which may have led to inaccuracy in surface area measurement, thereby making the comparison of results difficult.

The substantial increase in dividing algal cells under elevated pCO_2 (MI; Fig. 2c) is in accordance with previous studies reporting high MIs in anemones under high pCO_2[11,14]. It is important to note that there was no variation in algal genotype as the anemones from all three sites were found to harbor *Symbiodinium* type A19[12], excluding the possibility that genetic makeup of the *Symbiodinium* is responsible for the difference. The marked increase in algal division is most likely a direct result of massive CO_2 input, as *Symbiodinium* in anemones remain carbon limited under normal conditions[11,14,26,27]. Since cnidarians are required to maintain cell-specific densities of their algal symbionts to avoid toxicity from excess oxidative products[28], the host may initiate either active expulsion of symbionts and/or chemically-signaled arrest of algal reproduction[29]. Here, the high MIs but same algal densities, relative to algal densities at the control site, suggest that the anemones were unable to regulate algal repro-

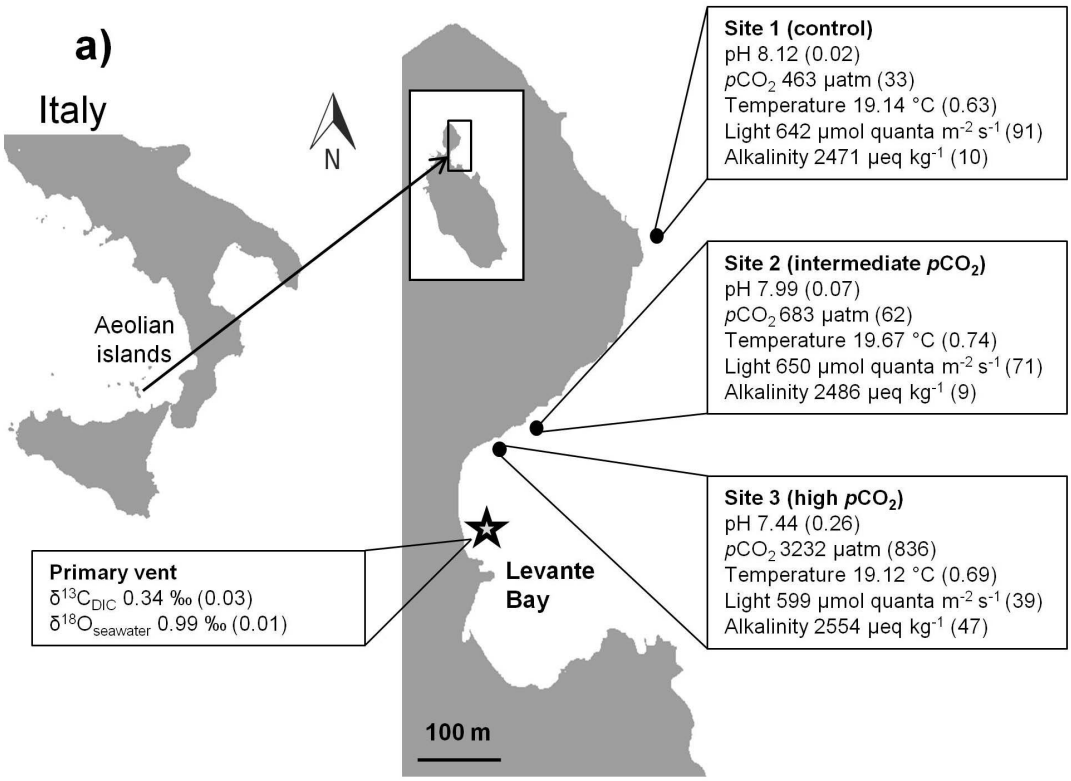

Figure 1 | General information on the study sites and the studied organism. (a) Map of the study area with sampling sites 1 (control), 2 (intermediate pCO_2) and 3 (high pCO_2). Boxes show mean values (±SD) of each site for: pH, pCO_2, temperature, light and alkalinity. $\delta^{13}C_{DIC}$ and $\delta^{18}O_{seawater}$ (‰) are presented for the primary vent site. The map was created in Adobe Illustrator CS3 (Adobe Systems Inc., San Jose, USA). (b) Image showing *A. viridis* at sampling site 3 (high pCO_2). Photo credit: M. F. (b).

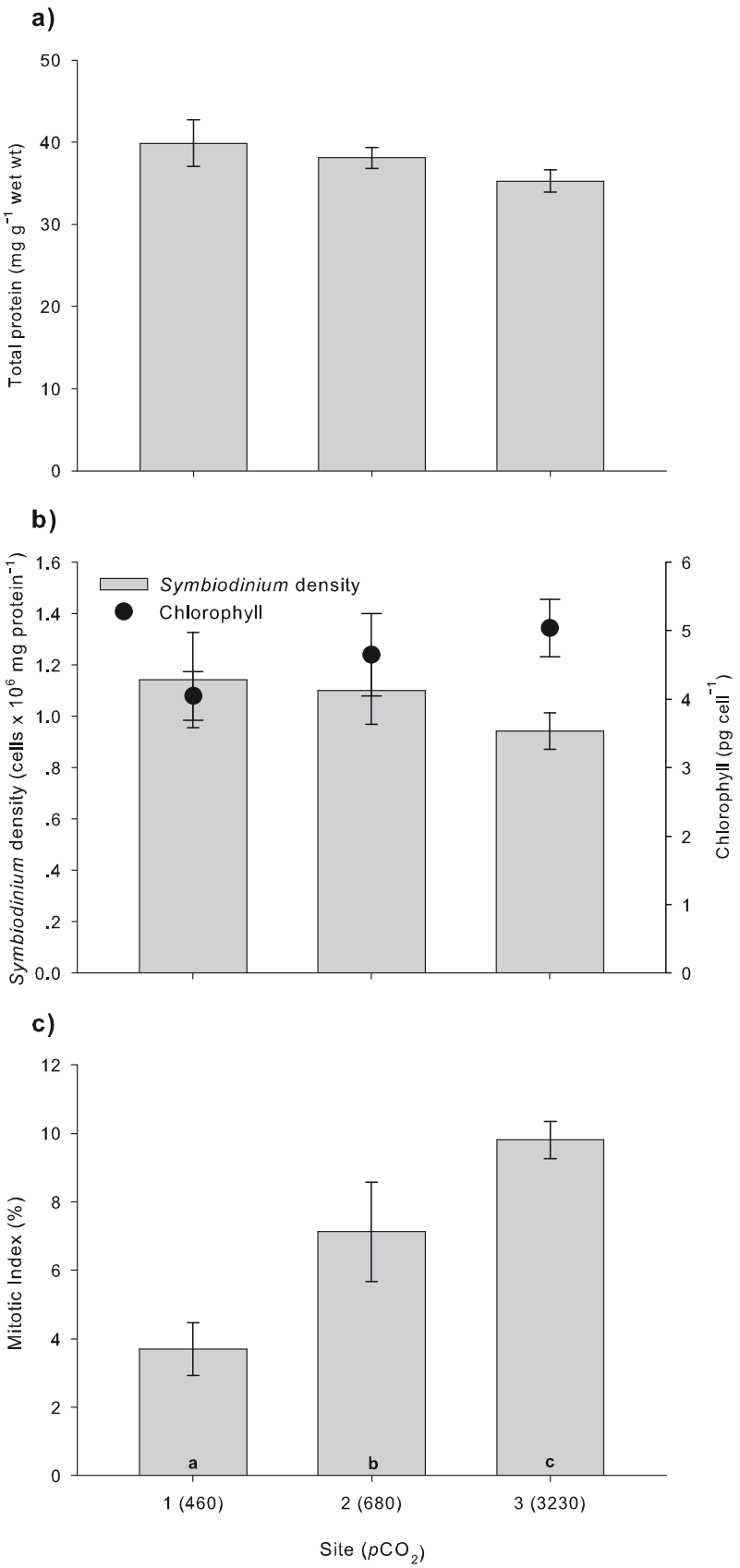

Figure 2 | Physiological parameter measurements of *A. viridis* from sites 1 (control), 2 (intermediate pCO_2) and 3 (high pCO_2). (a) Protein concentration (n = 16). (b) *Symbiodinium* density (bars) and chlorophyll concentration (circles) (n = 16). (c) Mitotic index (n = 8). Note that the mean pCO_2 (µatm; Table 1) is given in parentheses for each site. All data represent the mean ± SEM. *Letters* indicate significant differences between sites (Tukey, $P < 0.05$).

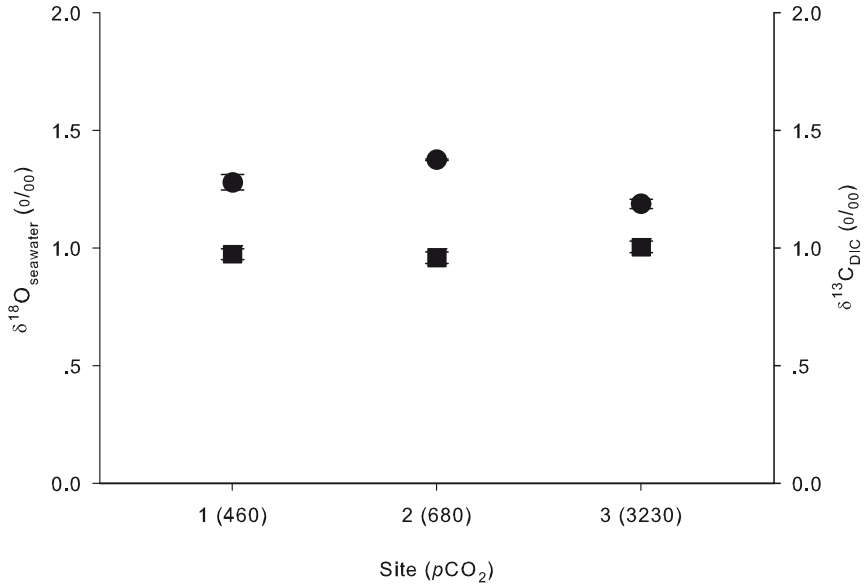

Figure 3 | Isotopic measurements of seawater at the sampling sites. $\delta^{13}C_{DIC}$ (circles) and $\delta^{18}O_{seawater}$ (squares) (‰) at sites 1 (control), 2 (intermediate pCO_2) and 3 (high pCO_2). Note that the mean pCO_2 (µatm; Table 1) is given in parentheses for each site. All values represent the mean ± SEM (n = 3).

duction under the elevated pCO_2 conditions and therefore densities were likely maintained through *Symbiodinium* expulsion. Considering that in addition iron (Fe) is the most important trace element for algal growth[30], Fe enrichment in the seawater near the vent site[13,31] may have also affected algal proliferation to some extent.

The acidification of seawater close to the venting source arises from the constant gas emissions[13]. In addition to total DIC increasing by 17% at the high pCO_2 site as compared to the control, $CO_{2(aq)}$ increased near the venting source (7-fold increase at the high pCO_2 site; see Table 1). Although the carbonate system still consists mostly of bicarbonate (94%), $CO_{2(aq)}$ increased from less than 1% at the control site to 4% at the high pCO_2 site (Table 1). Nonetheless, the isotopic composition of the inorganic carbon source in this area for the anemones appears to be constant as data shows that $\delta^{13}C_{DIC}$ does not change between sites (Fig. 3). Consequently, the pronounced and persistent depletion in ^{13}C in the tissues of *A. viridis* and its *Symbiodinium* close to the vent cannot be explained by the assimilation of a ^{13}C-depleted carbon source. The large increase in pCO_2 in the seawater (Table 1; Fig. 1a) and its availability for *A. viridis* most likely account for the decrease in *A. viridis* $\delta^{13}C$ values in both *Symbiodinium* and host tissue. The values near the vent (Fig. 4a, b) were well below the lower limit of the range reported previously for both tropical and subtropical sea anemones and *Symbiodinium*[32,33].

$\delta^{13}C_T$ values decreased at the intermediate and high pCO_2 sites to -17.62 ± 0.19‰ and -19.12 ± 0.16‰, respectively, as compared to the control site (-16.66 ± 0.2‰) (Fig. 4a), suggesting an increase in photosynthetically fixed carbon relative to heterotrophically acquired carbon in the host[20,34,35]. Taking seasonal and regional variability into account, average zooplankton and particulate organic carbon (POC) $\delta^{13}C$ values reported in the area for surface waters range between −21 and −22‰[36]. We assumed that the availability of these extrinsic carbon sources was constant across all sampling sites in our study, as the relatively short distance between sampling sites (<500 m) and their orientation in Levante Bay towards the open sea renders differences in food availability most unlikely as a factor. Based on mass balance estimation, our calculations show about 5% heterotrophic input to $\delta^{13}C_T$ at the control site (using $\delta^{13}C_T = -16.66$‰ and $\delta^{13}C_S = -15.1$‰, assuming

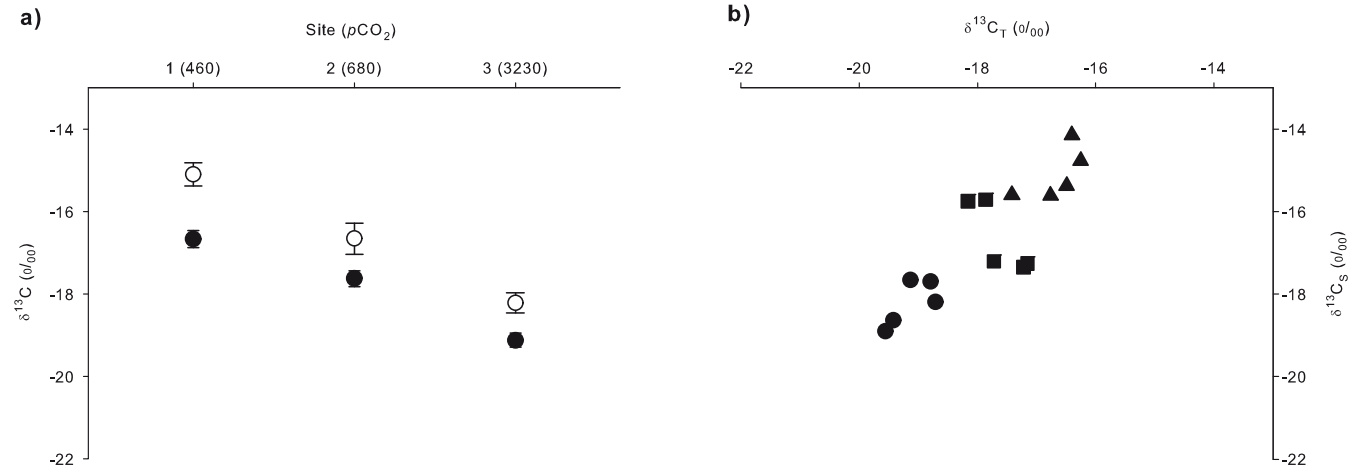

Figure 4 | $\delta^{13}C$ in *A. viridis* from sites 1 (control), 2 (intermediate pCO_2) and 3 (high pCO_2). (a) Mean $\delta^{13}C$ (‰) values (±SEM; n = 5) of *Symbiodinium* (white circles) and animal tissue (black circles). (b) $\delta^{13}C_T$ vs. $\delta^{13}C_S$ (‰) for individual *A. viridis* specimens from sites 1 (triangles), 2 (squares) and 3 (circles). Note that the mean pCO_2 (µatm; Table 1) is given in parentheses for each sampling site.

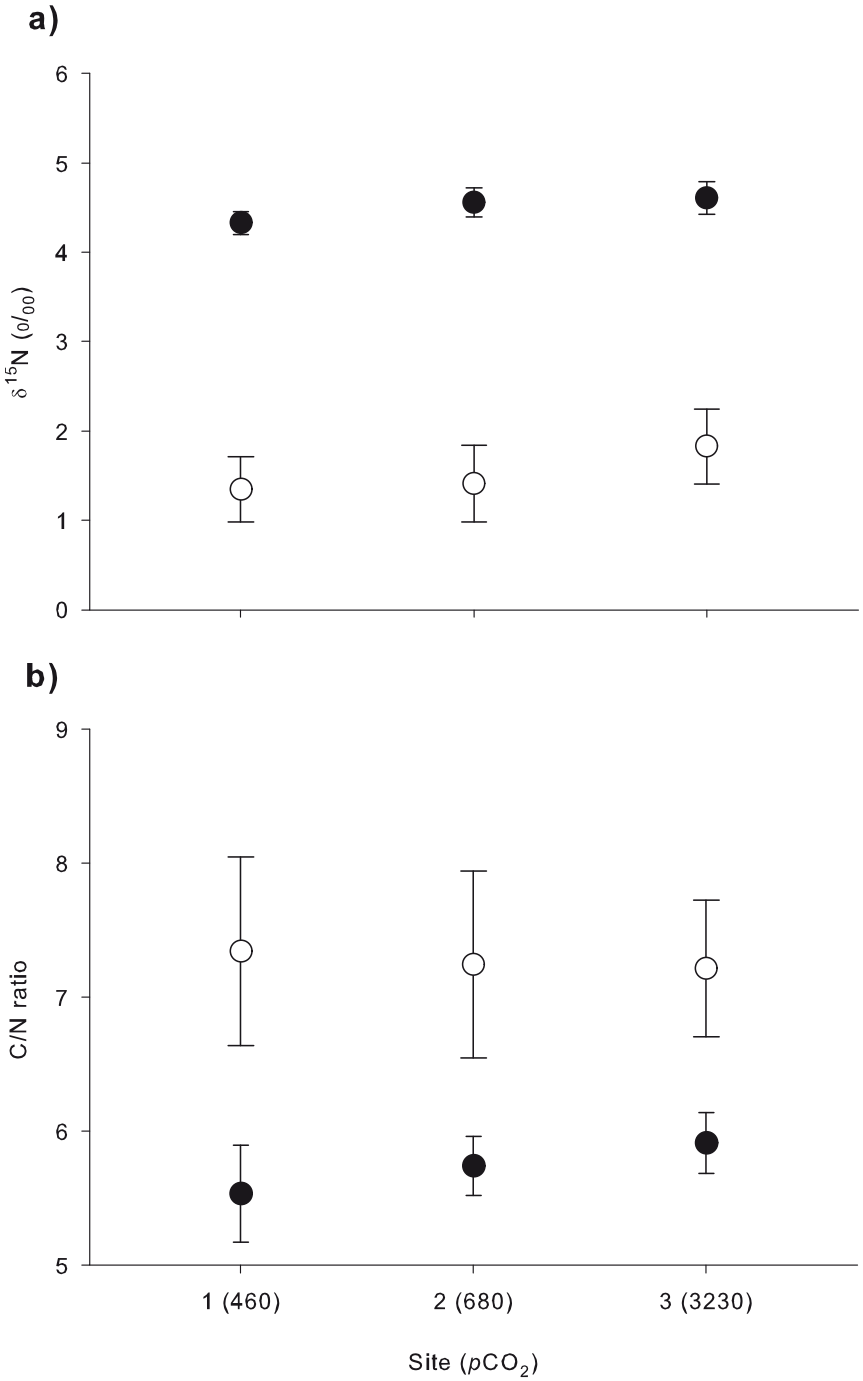

Figure 5 | $\delta^{15}N$ and C/N ratios in *A. viridis* from sites 1 (control), 2 (intermediate pCO_2) and 3 (high pCO_2). Measurements in *Symbiodinium* (white circles) and animal tissue (black circles) of: (a) $\delta^{15}N$ (‰), and (b) C/N ratio. Note that the mean pCO_2 (μatm; Table 1) is given in parentheses for each site. All values represent the mean ± SEM (n = 5).

$\delta^{13}C_{zooplankton/POC} = -22‰$). This is typical of cnidarian-algae symbioses, in which *Symbiodinium* may contribute up to 95% of their photosynthetically-produced carbon to the host[37]. Based on the same assumptions, at the high pCO_2 site the heterotrophic input to $\delta^{13}C_T$ reduced to about 2.5% (using $\delta^{13}C_T = -19.12‰$ and $\delta^{13}C_S = -18.21‰$, assuming $\delta^{13}C_{zooplankton/POC} = -22‰$), leading to a greater autotrophic input. This observation is also supported by the difference in $\delta^{13}C$ values between host tissue and *Symbiodinium*, which reflects the relative contribution of heterotrophy and photosynthesis to fixed carbon[20,38]. Cnidarian host tissue and *Symbiodinium* stable carbon isotopic values are usually within 2‰ of each other[20,39,40]. There was a significant reduction in $\delta^{13}C_S$-$\delta^{13}C_T$ with increasing pCO_2 from 1.56 ± 0.21‰ at the control site to 0.96 ± 0.31‰ and 0.9 ± 0.17‰ at the intermediate pCO_2 and high pCO_2 sites, respectively (Fig. 4a). This further indicates an increase in the autotrophic/heterotrophic ratio via translocated autotrophic carbon to the host.

Our results suggest that elevated pCO_2 near the vent promotes carbon isotope fractionation by *Symbiodinium* during photosynthesis, leading to lighter $\delta^{13}C_S$ values. $\delta^{13}C_S$ showed a substantial decrease from −15.1 ± 0.28‰ at the control site to −16.65 ± 0.37‰ and −18.21 ± 0.24‰ at the intermediate and high pCO_2 sites, respectively (Fig. 4a). Many studies have shown that $\delta^{13}C$ is depleted in marine photosynthetic organisms under elevated

Table 1 | Carbonate chemistry of seawater at sampling sites 1 (control), 2 (intermediate pCO_2) and 3 (high pCO_2). Parameters were calculated from pH_{NBS}, total alkalinity (TA), ambient seawater temperature, and salinity (38‰) using the program CO_2SYS[54]. All data shown are the mean (±SD). Dissolved inorganic carbon (DIC)

Site	pH_{NBS}	TA (μeq kg^{-1})	pCO_2 (μatm)	DIC (μmol kg^{-1})	$HC0_3^-$ (μmol kg^{-1})	CO_3^{2-} (μmol kg^{-1})	$CO_{2(aq)}$ (μmol kg^{-1})
1. Control	8.12 (0.02)	2554 (47)	463 (33)	2206 (22)	1998 (29)	193 (8)	15 (1)
2. Intermediate pCO_2	7.99 (0.07)	2486 (9)	683 (62)	2287 (46)	2113 (65)	152 (23)	22 (4)
3. High pCO_2	7.44 (0.26)	2501 (20)	3232 (836)	2585 (123)	2430 (93)	50 (25)	105 (53)

pCO_2[41–44]. Under normal conditions, the majority of *Symbiodinium* carbon requirements (~85%) are met via energy-demanding carbon-concentrating mechanisms (CCMs), whilst the remainder diffuses passively from seawater to the *Symbiodinium* cells[28]. When pCO_2 is elevated, $CO_{2(aq)}$ can replace HCO_3^- as the main carbon source for photosynthesis while energy-consuming CCMs become less important[43,45]. Form II ribulose 1,5-bisphosphate carboxylase/oxygenase (form II Rubisco), which is the carboxylating enzyme in *Symbiodinium*[46], discriminates against ^{13}C[47]. Enhanced levels of pCO_2 in the proximity of the vent diffuse to the Rubisco, which favors ^{12}C for carbon fixation and ultimately results in a lightning trend of $\delta^{13}C_S$ values. Krief *et al.* (2010) reported the same trend in two species of scleractinian corals after experimental exposure to high pCO_2 in a controlled pCO_2 system. While Krief *et al.* (2010) kept corals under elevated pCO_2 for a period of 14 months, our *in situ* study at the CO_2 vent site lends insight into a long-term exposure scenario[48].

$\delta^{15}N_T$ and $\delta^{15}N_S$ values did not change along the pCO_2 gradient, suggesting that the anemones' function and performance reside within normal bounds close to the vent after long-term exposure to acidification conditions (Fig. 5a). Further supporting this concept is the lack of change in C/N ratio between sites (Fig. 5b). The C/N ratio is considered a good proxy for an organism's condition since it reflects the ratio of lipids and carbohydrates to proteins[49]. The apparent absence of preferential accumulation/loss of lipids, carbohydrates or proteins in *A. viridis* in high pCO_2/low pH surroundings indicates therefore that the anemones were well acclimated.

Generally, animals exposed to high pCO_2/low pH have to compensate for acid-base imbalance in intra- and extracellular spaces thereby imposing elevated metabolic costs[50]. A recent study by Laurent *et al.* (2014) demonstrated the high capacity of *A. viridis* to regulate against decreases in internal and external pH, thereby maintaining normal cellular metabolism and physiology[51]. Our results indicate the adaptation and potential resilience of *A. viridis* to acidification conditions, as physiological data (i.e. protein content, *Symbiodinium* density and chlorophyll *a* concentration; Fig. 2a, b), along with $\delta^{15}N$ values and C/N ratios (Fig. 5a, b), remained unaffected among sites along the pCO_2 gradient. Moreover, the high pCO_2 environment probably stimulated cell division of algal symbionts (Fig. 2c).

We have shown that the anemone host relies more on photosynthetically derived carbon under elevated pCO_2. We propose that *A. viridis* optimizes energy utilization under elevated pCO_2 through an increased autotrophic input, although isotopic data show that heterotrophy is maintained as an additional source of energy/nutrients. These factors may contribute, at least in part, to the increased size and abundance of the *A. viridis* population proximate to the vent site as reported in a previous study[11]. In conclusion, increased autotrophic/heterotrophic ratio may enhance the competitive advantage of symbiotic anemones over other invertebrates and improve their ecological success in benthic communities. These are valuable findings that merit further study for predicting the performance of non-calcifying symbiotic cnidarians in future high-CO_2 oceans.

Methods

Study sites. This study was conducted along the sublittoral in Levante Bay, Vulcano Island (38° 25′ N, 14° 57′ E), part of the Aeolian Island chain, NE Sicily (Fig. 1a) in May 2012. Shallow-water CO_2 vents create a natural pCO_2/pH gradient along the north-easterly side of the bay, ranging from pH 6.05 to 8.29 at >350 m from the vent site[8,13].

Three sites were selected for animal sampling in accordance with previous studies (see Fig. 1a)[7,8,11,13]. Site 1 (control) was an ambient seawater reference station, located outside the vent area (>400 m); Site 2 (intermediate pCO_2) was ~300 m away from the CO_2 vents; Site 3 (high pCO_2) was in the proximity of the CO_2 vents (~260 m). Sampling at the primary vent site (indicated by the star symbol in Fig. 1a) was for collection of seawater samples only.

Carbonate chemistry and physical measurements. Seawater pH (NBS scale) and temperature were measured at all sites several times a day for 4 days using a pH meter (YSI Professional Plus, Handheld Multiparameter Instrument, USA). Water samples for total alkalinity (TA) analysis were collected from each site, cooled and stored in the dark until analysis. TA was quantified with a Metrohm 862 compact titrosampler[52]. The pCO_2 levels were calculated from salinity (=38‰, as reported by Johnson, 2012[53]) and TA and pH_{NBS} measurements using the program CO_2SYS [Pierrot, D. E., Lewis, E. & Wallace, D. W. R. MS Excel program developed for CO_2 system calculations. Carbon dioxide information analysis center, Oak Ridge National Laboratory, US Department of Energy, Oak Ridge, TN, USA (2006)], selecting the constants of Mehrbach *et al.* (1973)[54]. Carbonate chemistry parameters are shown in Table 1. Light intensity at each site was measured hourly for 3 consecutive days close to the seabed (1–2 m depth) with HOBO Pendant® Temperature/Light data loggers (Onset, Pocasset, MA, USA). The logged light data were converted from lux to μmol quanta m^2 s^{-1} (Fig. 1a)[55].

Sample collection in the field. *Anemones. A. viridis*, a dominant benthic organism in Levante Bay, was prevalent throughout the study area. Sixteen anemones were collected randomly from each site at a depth of 1–2 m and immediately frozen until further analyses. To minimize any confounding responses due to age and/or size all samples were of similar size (oral disc diameter of 2.5–3.5 cm)[56]. Between 5 and 10 tentacles were clipped from each anemone at every site (n = 16). Tentacles were processed for total protein and algal characteristics (i.e., *Symbiodinium* density, chlorophyll *a* concentration and mitotic index) at the sampling site. Samples were weighed (CT 1202, Citizen, accuracy 0.01 g) and homogenized in 0.2 μm sterile filtered seawater (FSW) with an electric homogenizer (DIAX 100 homogenizer Heidolph Instruments GmbH & Co. KG, Schwabach, Germany). The homogenate and all anemones were immediately frozen and then transported on dry ice to the Interuniversity Institute for Marine Sciences (IUI), Israel, where they were stored at −80 °C pending analyses.

Seawater. Seawater samples were collected from the four sites for carbon isotopes of dissolved inorganic carbon (DIC; $\delta^{13}C_{DIC}$) and oxygen isotopic analysis ($\delta^{18}O_{seawater}$). Triplicate samples for $\delta^{13}C_{DIC}$ analysis were immediately poisoned upon collection with 60 μl saturated solution of mercuric chloride and stored in 60 ml brown bottles at room temperature until analysis. Triplicate samples for $\delta^{18}O_{seawater}$ analysis were collected in 50 ml test tubes (Stardest) and stored at room temperature until analysis.

Total protein, *Symbiodinium* density, mitotic index and chlorophyll concentration. The tissue homogenate of each anemone (n = 16) was further processed and analyzed for measurements of physiological parameters. Total protein analysis was performed by removing 100 μl of the tissue homogenate and sonication on ice with a Branson Sonifier B12 (Branson Sonic Power Co., Danbury, Connecticut, USA) for 20 s. Quantification was done after Bradford (1976) using the Quick Start Bradford Protein Assay Kit and Quick Start Bovine Serum Albumin Standard Set (Bio-Rad Laboratories, Hercules, CA, USA)[57]. Optical density was read at 595 nm using an ELISA reader (Multiskan spectrum, Thermo Fisher Scientific Inc., USA).

For measurement of algal characteristics, 2 ml of homogenate of each sample (n = 16) were centrifuged (5000 rpm at 4°C; 4K15 centrifuge, Sigma) and re-suspended four times in FSW. Re-suspended *Symbiodinium* were used for chlorophyll *a* extraction in acetone (100%) at 4°C in the dark for 24 hours. Concentrations of chlorophyll *a* were measured using spectrophotometry (Ultrospec 2100 pro, GE Bioscience, USA) and calculated using standard equations[58]. Chlorophyll concentration was calculated per *Symbiodinium* cell. *Symbiodinium* densities were quantified from 4 replicate counts using a Neubauer haemocytometer and normalized to protein concentration. Mitotic index (MI) was measured as an indicator of *Symbiodinium* growth and was calculated as a percentage of doublets with a complete cleavage furrow observed per 1000 cells (n = 8 per sampling station)[59].

Separation of anemone tissue and *Symbiodinium* for isotope analysis. Subsamples of 250 mg were excised from the tentacles of each anemone (n = 5 per site) and placed in sterile 15 ml falcon tubes (Stardest). After adding 1 ml 0.2 μm filtered seawater (FSW), an electric homogenizer (DIAX 100 homogenizer Heidolph Instruments GmbH & Co. KG, Schwabach, Germany) was used to homogenize the tissue extract for 2 min. Separation of anemone tissue and *Symbiodinium* was done by the following protocol. The homogenate was centrifuged for 5 min at 5000 rpm (4K15 centrifuge, Sigma) to separate the algae (pellet) and the host tissue (supernatant). Visual inspections revealed no crossover of material between these components, but both were washed carefully.

The host supernatant was homogenized and centrifuged for 10 min at 13,500 rpm (4K15 centrifuge, Sigma, USA), resulting in pelleted host material for analysis. The *Symbiodinium* pellet was then re-suspended in 1 ml FSW, homogenized, and centrifuged for 5 min at 5000 rpm (4K15 centrifuge, Sigma, USA). The procedure was repeated twice in order to remove remaining tissue. All samples were washed with double-distilled water (DDW) to remove any remaining salts. Both the host tissue and *Symbiodinium* samples were dried with a lyophilizer (VirTis, Sentry 2.0, SP Scientific, USA) for 24 h for further isotopic analysis.

Stable isotope analyses. The isotopic measurements were made at the stable isotopes laboratory in the Department of Earth and Planetary Sciences, the Weizmann Institute of Science, Israel. The oxygen, carbon and nitrogen isotope measurements are reported in the conventional δ-notation.

Anemone tissue and Symbiodinium samples. $\delta^{13}C$ and $\delta^{15}N$ of 240–270 μg of dried tissue and algae were analyzed using an elemental analyzer (CE 1110) interfaced to the MAT 252 mass spectrometer. Long term precision of working standards for $\delta^{13}C$ is 0.05‰ and for $\delta^{15}N$ is 0.1‰ relative to V-PDB and Air respectively ($\pm 1\sigma$ SD). The carbon to nitrogen ratios (C/N) of anemone tissue and *Symbiodinium* were calculated from simultaneous %C and %N.

Seawater samples. $\delta^{18}O_{seawater}$ was analyzed by equilibrating 0.5 ml of samples with a mixture of 0.5% CO_2 in He at 25 °C for 24 h. The samples were analyzed on a Gas Bench II connected in-line to a Finigan MAT 252 mass spectrometer. The results are reported relative to VSMOW with 0.08‰ ($\pm 1\sigma$ SD) long-term precision of the laboratory working standards.

For $\delta^{13}C_{DIC}$ analysis, 1 ml sea water was injected into vials, flushed with He gas, acidified with 0.15 ml orthophosphoric acid (H_3PO_4) and left to react for 24 h at 25 °C. The samples were analyzed on a Gas Bench II and Finigan MAT 252. The results are reported relative to VPDB with 0.08‰ long-term precision ($\pm 1\sigma$ SD) of the $NaHCO_3$ laboratory standard.

Data analyses. All data was checked for normality using the Kolmogorov-Smirnov test and for homogeneity of variance using Cochran's test. In cases in which homogeneity of variance was achieved, we used one-way ANOVA and a multiple comparison test (Tukey). If homogeneity of variance or normality was not achieved, we used a non-parametric Kruskal-Wallis ANOVA and post-hoc Mann-Whitney U-tests for separation of significant factors. Differences between factors were considered significant for a P value < 0.05. Unless otherwise specified, mean values are presented $\pm$ standard error of mean (SEM). All data were analyzed using SPSS version 20 (SPSS IBM, New York, USA).

1. Hoegh-Guldberg, O. The adaptation of coral reefs to climate change: is the red 549 queen being outpaced? *Sci. Mar.* **76**, 403–408 (2012).
2. Intergovernmental Panel on Climate Change. In *Climate Change 2013: The Physical Science Basis. Contribution of Working Group I to the Fifth Assessment Report of the Intergovernmental Panel on Climate Change* [eds Stocker, T. F. *et al.*] (Cambridge Univ. Press, Cambridge, 2013).
3. Hall-Spencer, J. M. *et al.* Volcanic carbon dioxide vents show ecosystem effects of ocean acidification. *Nature* **454**, 96–99 (2008).
4. Kroeker, K. J., Micheli, F., Gambi, M. C. & Martz, T. R. Divergent ecosystem responses within a benthic marine community to ocean acidification. *Proc. Natl. Acad. Sci. USA* **108**, 14515–14520 (2011).
5. Meron, D. *et al.* Changes in coral microbial communities in response to a natural pH gradient. *ISME J.* **6**, 1775–1785 (2012).
6. Fabricius, K. E. *et al.* Losers and winners in coral reefs acclimatized to elevated carbon dioxide concentrations. *Nat. Clim. Change* **1**, 165–169 (2011).
7. Arnold, T. *et al.* Ocean acidification and the loss of phenolic substances in marine plants. *PLoS ONE* **7**, e35107 (2012).
8. Johnson, V. R. *et al.* Responses of marine benthic microalgae to elevated CO_2. *Mar. Biol.* **160**, 1813–1824 (2011).
9. Johnson, V. R., Russell, B. D., Fabricius, K. E., Brownlee, C. & Hall-Spencer, J. M. Temperate and tropical brown macroalgae thrive, despite decalcification, along natural CO_2 gradients. *Glob. Change Biol.* **18**, 2792–2803 (2012).
10. Calosi, P. *et al.* Distribution of sea urchins living near shallow water CO_2 vents is dependent upon species acid–base and ion-regulatory abilities. *Mar. Poll. Bull.* **73**, 470–484 (2013).
11. Suggett, D. J. *et al.* Sea anemones may thrive in a high CO_2 world.*Glob. Change Biol.* **18**, 3015–3025 (2012).
12. Borell, E. M., Steinke, M., Horwitz, R. & Fine, M. Increasing pCO_2 correlates with low concentrations of intracellular dimethylsulfoniopropionate in the sea anemone *Anemonia viridis*. *Ecol. Evol.* doi:10.1002/ece3.946 (2014).
13. Boatta, F. *et al.* Geochemical survey of Levante Bay, Vulcano Island (Italy), a natural laboratory for the study of ocean acidification. *Mar. Poll. Bull.* **73**, 485–494 (2013).
14. Towanda, T. & Thuesen, E. V. Prolonged exposure to elevated CO_2 promotes growth of the algal symbiont *Symbiodinium muscatinei* in the intertidal sea anemone *Anthopleura elegantissima*. *Biology Open* **1**, 615–621 (2012).
15. Bachar, A., Achituv, Y., Pasternak, Z. & Dubinsky, Z. Autotrophy versus heterotrophy: the origin of carbon determines its fate in a symbiotic sea anemone. *J. Exp. Mar. Biol. Ecol.* **349**, 295–298 (2007).
16. Brading, P., Warner, M. E., Smith, D. J. & Suggett, D. J. Contrasting modes of inorganic carbon acquisition amongst *Symbiodinium* (Dinophyceae) phylotypes. *New Phytol.* **200**, 432–442 (2013).
17. Dubinsky, Z. & Jokiel, P. L. Ratio of energy and nutrient fluxes regulates symbiosis between zooxanthellae and corals. *Pac. Sci.* **48**, 313–324 (1994).
18. Muscatine, L. *et al.* Stable isotopes ($\delta^{13}C$ and $\delta^{15}N$) of organic matrix from coral skeleton. *Proc. Natl. Acad. Sci. USA* **102**, 1525–1530 (2005).
19. Meron, D., Buia, M. C., Fine, M. & Banin, E. Changes in microbial communities associated with the sea anemone *Anemonia viridis* in a natural pH gradient. *Microbial Ecol.* **65**, 269–276 (2013).
20. Muscatine, L., Porter, J. W. & Kaplan, I. R. Resource partitioning by reef corals as determined from stable isotope composition. I. $\delta^{13}C$ of zooxanthellae and animal tissue vs depth. *Mar. Biol.* **100**, 185–193 (1989).
21. Rodrigues, L. J. & Grottoli, A. G. Calcification rate and the stable carbon, oxygen, and nitrogen isotopes in the skeleton, host tissue, and zooxanthellae of bleached and recovering Hawaiian corals. *Geochim. Cosmochim. Ac.* **70**, 2781–2789 (2006).
22. Reynaud, S. *et al.* Effect of light and feeding on the nitrogen isotopic composition of a zooxanthellate coral: role of nitrogen recycling. *Mar. Ecol. Prog. Ser.* **392**, 103–110 (2009).
23. Alamaru, A., Yam, R., Shemesh, A. & Loya, Y. Carbon and nitrogen utilization in two species of Red Sea corals along a depth gradient: Insights from stable isotope analysis of total organic material and lipids. *Geochim. Cosmochim. Ac.* **73**, 5333–5342 (2009).
24. Leal, M. C. *et al.* Trophic ecology of the facultative symbiotic coral *Oculina arbuscula*. *MEPS* **504**, 171–179 (2014).
25. Houlbrèque, F., Tambutté, E., Allemand, D. & Ferrier-Pagès, C. Interactions between zooplankton feeding, photosynthesis and skeletal growth in the scleractinian coral *Stylophora pistillata*. *J. Exp. Biol.* **207**, 1461–1469 (2004).
26. Jarrold, M. D. *et al.* Physiological plasticity preserves the metabolic relationship of the intertidal non-calcifying anthozoan–*Symbiodinium* symbiosis under ocean acidification. *J. Exp. Mar. Biol. Ecol.* **449**, 200–206 (2013).
27. Gibbin, E. M. & Davy, S. K. The photo-physiological response of a model cnidarian–dinoflagellate symbiosis to CO_2-induced acidification at the cellular level. *J. Exp. Mar. Biol. Ecol.* **457**, 1–7 (2014).
28. Furla, P. *et al.* The symbiotic anthozoan: a physiological chimera between alga and animal. *Integr. Comp. Biol.* **45**, 595–604 (2005).
29. Baghdasarian, G. & Muscatine, L. Preferential expulsion of dividing algal cells as a mechanism for regulating algal-cnidarian symbiosis. *Biol. Bull.* **199**, 278–286 (2000).
30. Falkowski, P. G., Barber, R. T. & Smetacek, V. Biogeochemical controls and feedbacks on ocean primary production. *Science* **281**, 200–206 (1998).
31. Horwitz, R., Borell, E. M., Fine, M. & Shaked, Y. Trace element profiles of the sea anemone *Anemonia viridis* living nearby a natural CO_2 vent. *Peer J* **2**, e538 (2014).
32. Bergschneider, H. & Muller-Parker, G. Nutritional role of two algal symbionts in the temperate sea anemone *Anthopleura elegantissima* Brandt. *Biol. Bull.* **215**, 73–88 (2008).
33. Cleveland, A., Verde, E. A. & Lee, R. W. Nutritional exchange in a tropical tripartite symbiosis: direct evidence for the transfer of nutrients from anemonefish to host anemone and zooxanthellae. *Mar. Biol.* **158**, 589–602 (2011).
34. Swart, P. K., Leder, J. J., Szmant, A. & Dodge, R. E. The origin of variations in the isotopic record of scleractinian corals: II. Carbon. *Geochim. Cosmochim. Ac.* **60**, 2871–2886 (1996).
35. McConnaughey, T. A., Burdett, J., Whelan, J. F. & Paull, C. K. Carbon isotopes in biological carbonates: respiration and photosynthesis. *Geochim. Cosmochim. Ac.* **61**, 611–622 (1997).
36. Mazzola, A. *et al.* Origin and distribution of suspended organic matter as inferred from carbon isotope composition in a Mediterranean semi-enclosed marine system. *Chem. Ecol.* **16**, 215–238 (1999).
37. Muscatine, L. Productivity of zooxanthellae. In *Primary Production in the Sea* [Falkowski, P. G. (ed.)] [649–658] (Plenum, New York, , USA, 1980).
38. Swart, P. K. *et al.* The isotopic composition of respired carbon dioxide in scleractinian corals: implications for cycling of organic carbon in corals. *Geochim. Cosmochim. Ac.* **69**, 1495–1509 (2005).
39. Reynaud, S. *et al.* Effect of feeding on the carbon and oxygen isotopic composition in the tissues and skeleton of the zooxanthellate coral *Stylophora pistillata*. *Mar. Ecol. Prog. Ser.* **238**, 81–89 (2002).
40. Grottoli, A. G., Rodrigues, L. J. & Juarez, C. Lipids and stable carbon isotopes in two species of Hawaiian corals, *Porites compressa* and *Montipora verrucosa*, following a bleaching event. *Mar. Biol.* **145**, 621–631 (2004).

41. Rau, G. H., Takahashi, T., Desmarais, D. J., Repeta, D. J. & Martin, J. H. The relationship between $\delta^{13}C$ of organic matter and $[CO_2]_{(aq)}$ in ocean surface water – data from a JGOFS site in the northeast Atlantic Ocean and a model. *Geochim. Cosmochim. Ac.* **56**, 1413–1419 (1992).
42. Laws, E. A., Popp, B. N., Bidigare, R. R., Kennicutt, M. C. & Macko, S. A. Dependence of phytoplankton carbon isotopic composition on growth rate and $[CO_2]_{(aq)}$ – theoretical considerations and experimental results. *Geochim. Cosmochim. Ac.* **59**, 1131–1138 (1995).
43. Erez, J., Bouevitch, A. & Kaplan, A. Carbon isotope fractionation by photosynthetic aquatic microorganisms: experiments with *Synechococcus* PCC7942, and a simple carbon flux model. *Can. J. Bot.* **76**, 1109–1118 (1997).
44. Vizzini, S. *et al.* Effect of explosive shallow hydrothermal vents on $\delta^{13}C$ and growth performance in the seagrass *Posidonia oceanica*. *J. Ecol.* **98**, 1284–1291 (2010).
45. Goericke, R. & Fry, B. Variations of marine plankton $\delta^{13}C$ with latitude, temperature, and dissolved CO_2 in the world ocean. *Global Biogeochem. Cy.* **8**, 85–90 (1994).
46. Mayfield, A. B., Hsiao, Y. Y., Chen, H. K. & Chen, C. S. Rubisco expression in the dinoflagellate *Symbiodinium* sp. is influenced by both photoperiod and endosymbiotic lifestyle. *Mar. Biotechnol.* **16**, 371–384 (2014).
47. Raven, J. A. Inorganic carbon acquisition by marine autotrophs. *Adv. Bot. Res.* **27**, 85–209 (1997).
48. Krief, S. *et al.* Physiological and isotopic responses of scleractinian corals to ocean acidification. *Geochim. Cosmochim. Ac.* **74**, 4988–5001 (2010).
49. Bodin, N., Le Loc'h, F. & Hily, C. Effect of lipid removal on carbon and nitrogen stable isotope ratios in crustacean tissues. *J. Exp. Mar. Biol. Ecol.* **341**, 168–175 (2007).
50. Fabry, V. J., Seibel, B. A., Feely, R. A. & Orr, J. C. Impacts of ocean acidification on marine fauna and ecosystem processes. *ICES J. Mar. Sci.* **65**, 414–432 (2008).
51. Laurent, J. *et al.* Regulation of intracellular pH in cnidarians: response to acidosis in *Anemonia viridis*. *FEBS J.* **281**, 683–695 (2014).
52. Cohen, S. Measuring gross and net calcification of a reef coral under ocean acidification conditions: methodological considerations. MSc Thesis. Bar-Ilan University, Israel (2011).
53. Johnson, V. R. A study of marine benthic algae along a natural carbon dioxide gradient. PhD Thesis. University of Plymouth, UK (2012).
54. Mehrbach, C., Culberson, C. H., Hawley, J. E. & Pytkowicz, R. M. Measurement of the apparent dissociation constants of carbonic acid in seawater at atmospheric pressure. *Limnol. Oceanogr.* **18**, 897–907 (1973).
55. Thimijan, R. W. & Heins, R. D. Photometric, radiometric, and quantum light units of measure: a review of procedures for interconversion. *HortScience* **18**, 818–822 (1983).
56. Perez, S. F., Cook, C. B. & Brooks, W. R. The role of symbiotic dinoflagellates in the temperature-induced bleaching response of the subtropical sea anemone *Aiptasia pallida*. *J. Exp. Mar. Biol. Ecol.* **256**, 1–14 (2001).
57. Bradford, M. M. A rapid and sensitive method for the quantification of microgram quantities of protein utilizing the principle of protein-dye binding. *Anal. Biochem.* **72**, 248–254 (1976).
58. Jeffrey, S. W. & Humphrey, G. F. New spectrophotometric equations for determining chlorophylls *a*, *b*, c_1 and c_2 in higher plants, algae and natural phytoplankton. *Biochem. Physiol. Pfl.* **167**, S191–S194 (1975).
59. Wilkerson, F. P., Muller-Parker, G. & Muscatine, L. Temporal patterns of cell division in natural populations of endosymbiotic algae. *Limnol. Oceanogr.* **28**, 1009–1014 (1983).

Acknowledgements

Thanks to Marco Milazzo (University of Palermo) for essential academic and logistical support. We are grateful to Gabriela Perna for help with the physiological parameter analyses. This study was funded in part by the FP7 ASSEMBLE project no. 227799, the EU MedSeA project, and an Israel Science Foundation grant to M.F.. E.M.B. was funded by the Minerva fellowship program.

Author contributions

R.H., E.M.B. and M.F. conceived the overall project. R.H. and E.M.B. conducted the field and laboratory work and analysed data. R.Y. and A.S. carried out stable isotope analyses. All authors reviewed and edited the manuscript.

Additional information

Competing financial interests: The authors declare no competing financial interests.

How to cite this article: Horwitz, R., Borell, E.M., Yam, R., Shemesh, A. & Fine, M. Natural high pCO_2 increases autotrophy in *Anemonia viridis* (Anthozoa) as revealed from stable isotope (C, N) analysis. *Sci. Rep.* 5, 8779; DOI:10.1038/srep08779 (2015).